J Mater Sci (2020) 55:480–497

Review

Review of photoreduction and synchronous patterning of graphene oxide toward advanced applications

Haobo Jiang[1], Bo Zhao[2,3], Yan Liu[1,*], Shuyi Li[1], Juan Liu[1], Yunyun Song[1], Dandan Wang[4,*], Wei Xin[2,*], and Luquan Ren[1]

[1] The Key Laboratory of Bionic Engineering Ministry of Education, Jilin University, Changchun 130023, China
[2] The Guo China-U.S. Photonics Laboratory, Changchun Institute of Optics, Fine Mechanics, and Physics, Chinese Academy of Sciences, Changchun 130033, China
[3] Department of Electronic Information and Physics, Changzhi University, Changzhi 046011, Shanxi, China
[4] GLOBALFOUNDRIES (Singapore) Pte. Ltd, 60 Woodlands Industrial Park D, Street 2, Singapore 738406, Singapore

Received: 8 June 2019
Accepted: 28 August 2019
Published online: 16 September 2019

ABSTRACT

In view of the bulk production, resolvability, dispersibility of aqueous solution, graphene oxides (GO) prepared by strong chemical oxidation of graphite flakes have been widely used for the production of graphene-like materials. However, because of the insulating nature caused by amounts of defects on its surface, the application of GO material is greatly constrained. Hence, effective reduction of GO becomes critical. The photoreduction of GO showed more attractive properties than conventional thermal/chemical routes due to its synchronous reduction and flexible patterning, which facilitates a number of applications, such as the electrochemical energy storage devices, electronic devices, and biomimetic substrates. In this review, we dedicatedly summarized the latest advances in photoreduction including the fabrications and applied values in multiple fields. We deem that the photoreduction and synchronous patterning of GO will have very prospects in the development of graphene devices.

Introduction

Ever since the first mechanical peeling of graphite in 2004, the two-dimensional (2D) carbon crystal with 0.34 nm thickness, named graphene, has raised much concern [1–4]. Subsequently, a series of exceptional physical/chemical properties (e.g., high carrier mobility [5, 6], optical transmittance [7, 8], pyroconductivity [9, 10], Young's modulus [11, 12], electrical conductivity [13, 14], flexibility [15, 16], stability [17, 18], and biocompatibility [19–21]) have been successfully discovered, which leads to a great upsurge in research interests with respect to graphene and its related materials [22, 23]. The research not only focuses on the intrinsic properties of materials, but also on the application potentials in the field of electrochemical (EC) energy storage [24, 25], electronics [26, 27], mechanics [28, 29] and even tissue engineering [30, 31]. The common preparations include the mechanical exfoliation [32–34], chemical

Address correspondence to E-mail: lyyw@jlu.edu.cn; DANDAN.WANG@globalfoundries.com; weixin@ciomp.ac.cn

https://doi.org/10.1007/s10853-019-03981-z

vapor deposition (CVD) [35, 36], epitaxial growth [37, 38] and ultrasonic exfoliation in 1-methyl-2-pyrrolidinone (NMP) [39, 40]. Nevertheless, all of these methods suffer from complex procedures or low yields, which more or less limit the wide applications of graphene in various scientific fields [41, 42].

As an alternative choice, graphene oxides (GOs), which could be considered as defective graphene with abundant oxygen-containing groups (OCGs) such as hydroxyl, carboxyl and epoxy, show several advantages that are of great benefit to practical applications [43, 44]. For instance, the GO can be produced on a large scale; it is possible to functionalize with various organic groups through covalent grafting [45–47]; the solution processing capability makes it tractable [48–50]. However, GO also has some drawbacks. The OCGs destroy the motion path of electron seriously and make GO dielectric, which significantly affects its application in electronics [51–53].

To partially restore the conductivity, research efforts have been devoted to find suitable methods that could be used for GO reduction. Typically, two kinds of methodologies with chemical [54–56] and thermal methods [57–59] have been successfully developed. The former needs the chemical reduction materials such as the hydrous ammonia, hydrazine and ascorbic acid, whereas the latter depends on high-temperature reaction environment [60]. Although the fact that these two methods make it possible to obtain reduced GO (RGO) with certain conductivity, practical issues with respect to the energy consumption, usage of toxic chemicals and dependence of special instruments significantly limits the applications. Compared with the aforementioned traditional reduction methods, recently the unique superiorities of irradiation processing technique of RGO along with the adjustable multi-parameter and patterning operation make the so-called photoreduction exhibit higher development prospects. This review summarizes the recent research progress of optical strategies that are capable of making RGO patterns through photoreduction processes, and it laid emphasis on its unique advantages in various fields. Although many challenges need to be faced at the present stage, for example, it is difficult to prepare high-quality graphene with less OCGs and defects, the controllability and flexibility have still revealed growth potential for widespread applications.

Photoreduction methods

Generally, according to the different reduction mechanism, the photoreduction of GO could be roughly categorized into photothermal (PT) and photochemical (PC) effects [61–63]. The PT effect is common since GO would adsorb light with a broad range of wavelength. But when the photon energy is so large it that triggers a chemical reaction, OCGs could be eliminated through the PC route [64, 65]. In this section, we do not pay attention to these mechanism but focus on the photoreduction and patterning methods according to the processing features, in which they are simply categorized into mask-free direct laser writing (DLW) and common irradiation with the help of shadow masks. To make the statement clearer, we will first introduce the properties of photoreduced graphene and then present a detailed introduction of the photoreduction methods on the basis of illumination wavelengths.

Characterization of the photoreduced graphene

Graphene oxide is a highly oxidized graphene sheet, which is decorated by plenty of OCGs. Under the photoreduction along with the removing the OCGs, the chemical composition and geometrical shape of the GO sheets can be changed simultaneously, resulting in the significant alteration in physical/chemical properties. However, due to the different preparation process, reduction degree and the raw graphite materials, the specific properties in independent photoreduced samples exist individual differences. As an example, we show a comparison of the characteristic performance of GO paper before and after solar irradiation [66]. The detailed experimental process is shown below.

As shown in Fig. 1, the RGO side of the GO/RGO paper and the pristine GO paper were characterized from X-ray diffraction (XRD), Raman spectroscopy, Fourier transform infrared (FTIR), resistance and X-ray photoelectron spectroscopy (XPS), respectively. The diffraction peak of pristine GO paper is at $2\theta = 11.8°$ (Fig. 1a). After the sunlight photoreduction, the peak disappears, predicating removal of OCGs. From the Raman spectroscopy (Fig. 1b), the I_D/I_G ratio of RGO sample shows a larger value than that of pristine GO, which is interpreted as some OCGs have been removed after photoreduction, but

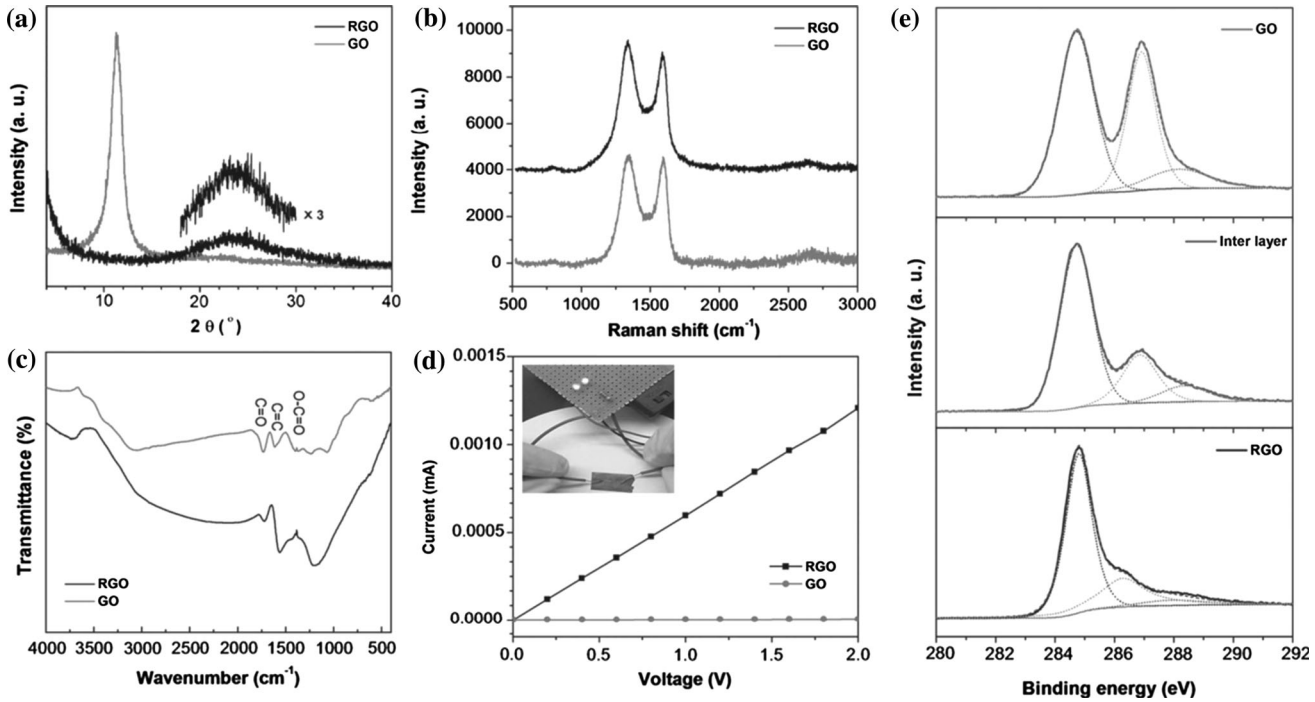

Figure 1 Characterization of GO and the photoreduced graphene (RGO) paper. **a** XRD patterns, **b** Raman spectra, **c** FTIR spectra of the pristine GO paper and RGO side of the GO/RGO film. **d** Current–voltage (*I–V*) characteristics of the GO and RGO papers (2 mm × 5 mm), the inset is a photograph of RGO paper lighting a bubble. **e** C1s XPS of the GO, the interlayer and the RGO. Reprinted with permission from [66], copyright (2015) Wiley-VCH.

at the same time there are some small fragments of GO that exist. This leads to a slight improvement in the defects of the material after reduction. As another characteristics method to identify the changes of chemical components after photoreduction, the FTIR spectra are also measured (Fig. 1c). Most transmission bands of OCGs have been eliminated after photoreduction, which also suggests the effective removal of OCGs. The electrical conductivity of the membrane material to a certain extent has been restored after reduction of sunlight due to the removal of some OCGs. The resistance of the pristine GO paper (2 mm × 5 mm) was measured to be ca. $4.1 \times 10^8\ \Omega$, whereas the resistance of RGO side decreased to $1.66 \times 10^6\ \Omega$ (Fig. 1d). Furthermore, the XPS measurements of GO side, interlayer and the RGO side was tested (Fig. 1e). From the XPS results, we find that the C/O mass ratio of GO side is lowest which is about the same as the pristine GO paper. The C/O mass ratio of the RGO side increased due to the removal of OCGs, and the ratio at interlayer of GO/RGO paper was between the GO and RGO sides.

The photoreduction and patterning of GO

The light source used in photoreduction can be a laser or the ordinary electro-magnetic radiation. Both the PT and PC effects can be considered during this process [61–63]. As a powerful tool for designable reduction and synchronous patterning, the mask-free DLW technology is undoubtedly a preferred choice [67, 68]. Whereas if an ordinary light source is considered, the photoreduction process may be more flexible. GO could be reduced either in aqueous solution or in the form of a solid film [69–71]. The RGO patterns can also be prepared with the help of shadow masks. In this part, the advance in photoreduction of GO is summarized according to different laser wavelengths.

Ultraviolet (UV) photoreduction of GO

The UV light irradiation is a common method for photoreduction. To GO, getting enough energy from outside is a better avenue to remove the OCGs and restore the sp2 domains. The UV radiation with high power can provide enough energy to the acceptor to

induce the generation of electron hole pairs. Many outcomes can be demonstrated from the perspective of experiments; UV light irradiation can effectively reduce GO [72, 73].

Excimer laser with the wavelength of 248 nm is the representative UV laser that can trigger GO reduction. Using this method, Orlando et al. first reduced GO to shaggy multilayer graphene with the C/O ratio of 40 [74]. The resistance is $\sim$ 100–500 Ω sq^{-1} [75]. Figure 2a–c exhibits the typical scanning electron microscope (SEM) images of GO before (smooth) and after (rough with abundant edges) laser reduction. The inset is the Raman mapping of the G peak at 2672 cm^{-1} as a function of XY position, which indicates the reduction of GO in the irradiated regions. As compared with other laser sources, the excimer laser is capable of thorough reduction of GO. This reduction permits making both microscale and macroscopic patterns. The resultant RGO shows highly porous structures, and it promotes the applications in EC energy storage devices.

To achieve patterning of high-throughput photoreduction on large-area GO films with nanometer resolution, Prezioso et al. first made patterns over large areas ($\sim$ 10 mm^2) with sub-micrometer resolution via spatially resolved photoreduction by direct high-throughput resistless extreme-UV (EUV, 46.9 nm) laser exposure (Fig. 2d) [76]. The GO stripe patterns with 2 μm periodicity were obtained through modulating irradiated optical path of the EUV with the help of a Lloyd's interferometer (Fig. 2e). The entire EUV range is below the energy threshold of photoreduction of GO ($\approx$ 3.2 eV, $\lambda < \approx$ 390 nm) that causes the conjugated structures breaking [77]. It has been proved to be an ideal choice to fabricate graphene-based devices with high-resolution flexible patterns, and this technique will exceed the resolution limit of ultraviolet radiation in standard lithography.

Another representative reduction and patterning of GO was reported by Sun's group using the two-beam-laser interference (TBLI) technique. A standard single-mode Nd:YAG laser (Spectra-Physics, 355 nm, 10 Hz and 10 ns pulse duration) was used as the light source. By splitting the incident laser into two beams and then focusing them at one point, the optical field

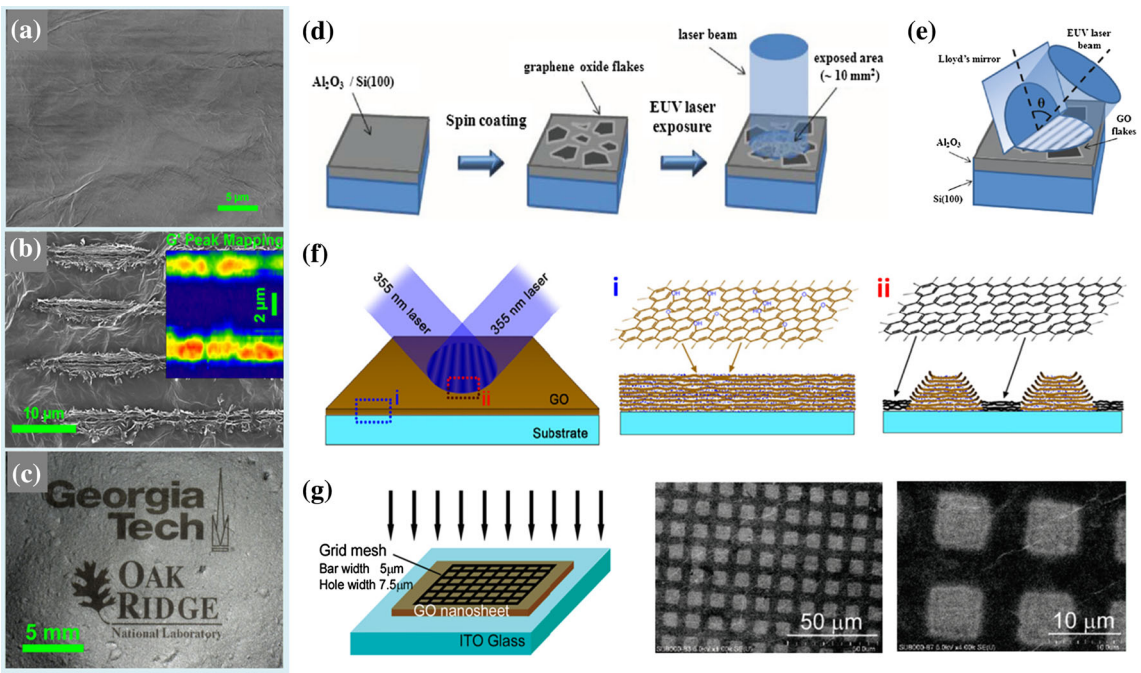

Figure 2 The UV photoreduction of GO. Typical SEM images of GO before (**a**) and after (**b**) excimer laser irradiation in high vacuum. The inset is the Raman mapping of G peak at 2672 cm^{-1}. **c** Photographs of RGO Logos. Reprinted with permission from [74], copyright (2013) Elsevier Ltd. Schematic diagrams of photoreduction (**d**) and patterning (**e**) using EUV laser exposure. Reprinted with permission from [76], copyright (2012) American Chemical Society. **f** Illustration of TBLI reduction of GO film. Reprinted with permission from [78], copyright (2012) Elsevier Ltd. **g** Schematic diagram and SEM images of photopatterning using the high-pressure Hg lamp. Reprinted with permission from [79], copyright (2010) American Chemical Society.

distribution with high-resolution interference fringes can be obtained [78]. Grating-like periodic GO structures with nanoscale roughness has been fabricated during the laser processing process (Fig. 2f). The OCGs have been reduced during the laser interference process; in the high-laser-intensity region, the OCGs were the most thoroughly restored, and in the low intensity region the OCGs were to be preserved in part. Additionally, during the photoreduction, there exist both PT reaction and PC action. Laser-induced PT action causes part of OCGs to come out, also accompanied by ablation of graphene sheets by laser cutting. The existence of these two roles forms a special periodic graphene patterning.

Except for the photoreduction using laser, Matsumoto et al. [79] also reported a research using a 500 W high-pressure Hg lamp in H_2 or N_2 atmosphere (Fig. 2g). This method can significantly remove OCGs and partially restore sp^2 domains. Due to the PC process of photoreduction, the surface temperature of GO material generally does not exceed 40 °C, which can avoid PT effects and allow micrometer size patterning with relatively flat topography. This UV light reduction technology is a relatively simple photoreduction technology requiring mild operating environment. Thus, it will extend the multitudinous applications of GO.

Visible photoreduction of GO

The photoreduction of GO using visible irradiation is the most common method because of its visibility, effectiveness and easy operation. As mentioned above, visible photoreduction process is quite different the UV operation in principle. Irradiation of the sample at a longer wavelength allows it to absorb enough light energy and obtain higher heat, so the PT effect is more pronounced during this process.

The difference in the photoreduction by incident light at different wavelengths was first studied by Sokolov et al. [80]. They compared the features of graphene by Raman spectroscopy via continuous-wave (CW, 532 nm) or pulsed (532 and 355 nm) laser excitation of GO in air atmosphere and N_2, respectively (Fig. 3a). For graphene materials, Raman spectroscopy is a convenient and rapid method to detect and analyze the information of graphene layer number, defect degree, doping condition and so on [81–85]. In experiment, it was found that the G peak of the material in the irradiated area using 532 nm CW laser was the narrowest in N_2, indicating that the reduction at this time was the best. Compared with the reduction of pulsed laser, the results also show that the existence of D peak, that is, the reduction degree depends on the output form of laser.

Diode laser could remove OCGs and patterning of GO all at once. Teoh et al. reported a method to create 3D rGO–GO–rGO stacked-layered structures with micropatterns defined in each layer through using of focused diode laser beam (532 nm) to reduce GO and appropriate controlling of laser temperature on the spin coating substrate of rGO patterning (Fig. 3b) [85]. Zhou et al. [87] used diode laser "direct-write" technique to reduce GO with patterns through laser cutting effect, and in his experiment he used laser wavelength of 663 nm (Fig. 3c). Amount of thermal energy has been produced by laser cutting effect, so that the GO film (> 5 layers) can absorb heat to raise its temperature to the threshold of evaporation, while causing the reduction and combustion of GO film in air. It can be predicted that this method of reduction and patterning can achieve more precise control by optimizing parameters like the choosing high-thermal conductivity-based material and regulating the temperature of the substrate which equal to the energy of the laser.

Additionally, to effectively remove the OCGs on GO sheets, a xenon discharge tube assembled on a camera has been applied. As typical delegates, Cote et al. [61] first reported the reduction and patterning of GO by flash lamp under ambient conditions. Xenon flash bulbs can provide visible light (> 400 nm). For an ordinary camera flash unit, it can offer 0.1–2 J cm^{-2} of energy per pulse at short range (< 2 mm), according to the optical absorption of GO in the visible range (400–800 nm, ~ 63–1260 mJ/m^2). Based on the thermal analysis, thermal energy of 70 mJ can heat the GO film to 100 °C. So the enough energy provided by a single exposure of the flash can induce an effective reduction of GO (Fig. 3d). This shows many unique advantages, for instance, GO could be rapidly reduced upon flash treatment; an expanded RGO structure would be formed due to the emission of carbon species, which could significantly increase the surface area and reveal great potential in EC energy storage applications. Later, Gilje et al. [62] investigated the flash-induced PT reduction of GO for large-area array patterning and combustion applications. Figure 3e shows a comparison of photograph and SEM images before and after the

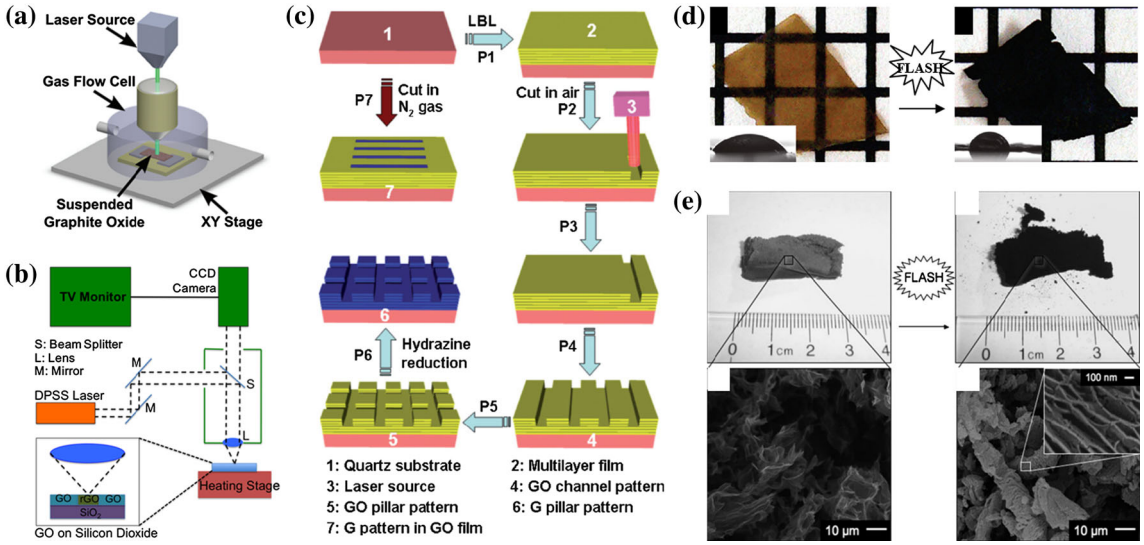

Figure 3 The visible photoreduction of GO. **a**–**c** Schematic diagram of different setup for visible laser reduction of GO. Respectively, reprinted with permission from [80, 86, 87], copyright (2010) American Chemical Society (2012) American Institute of Physics and (2010) Wiley-VCH. **d**, **e** Photograph and SEM image comparisons of GO before and after flash reduction. Respectively, reprinted with permission from [61] and [62], copyright (2009) American Chemical Society and (2010) Wiley-VCH.

photoreduction of GO foam. After flash treatment, the exfoliated layers of graphene were leaving.

Near-infrared (NIR) photoreduction of GO

The PT effect of NIR photoreduction is more obvious, and the energy requirement for light is higher. In this segment, we will mainly recommend three representative works using laser including the LightScribe technology (788 nm), femtosecond laser direct writing (FsLDW, 790 nm) and picosecond pulsed laser irradiation (1064 nm). For LightScribe technology, it was first invented by Hewlett-Packard Company for the preparation of labels and patterns on optical disks [88]. Then it was reported by the Kaner's group for photoreducing and flexible patterning of GO toward all graphene devices (Fig. 4a) [89]. In general, to the graphene devices prepared by LightScribe method, first the GO film is coated on a flexible, transferable substrate and then fixed to cover on the specific LightScribe-enabled digital video disk (DVD), dielectric disk. The film was photoreduced by the NIR laser in DVD driver. According to computer predesign, graphene images with high grayscale resolution have been generated simultaneously. While removing most of the OCGs on the GO layer to enhanced conductivity up to 1738 S m^{-1}, the low-power NIR photoreduction can change the surface topography of GO to form porous structures with high specific surface area (1520 m^2 g^{-1}), which is benefits to store energy for carriers and reveals application prospects in the field of EC. This technique is low-cost and environment-friendly and brings the development of graphene-based electronics.

Another work using the FsLDW technology (790 nm, 120 fs) for GO reduction was first reported by Zhang et al. [90]. The laser is concentrated by 100× objective lens (NA = 1.4). When the GO is processed, the exposure time is adjusted to unit voxel 600 μs and the laser scanning step length is 100 nm. This innovative progress developed a novel method to fabricate micro-current patterns on GO films (Fig. 4b). Soon afterward, in 2014, their team reported a method of programmable N-doping and reduction of GO, which was realized by the FsLDW technique in the ammonia atmosphere of the microcavity (Fig. 4c) [91]. Doping is widely used to tailor the energy band structures of bulk and nanoscale materials, facilitating the construction of various multifunctional materials and devices [92–94]. The unique method allows fine control of the doped region, so it is possible to make complex patterns with high resolution on multiple substrates. Figure 4c shows the atomic force microscope (AFM) images of an araneose RGO micropattern. It can be found that the film of GO has been reduced ~ 30 nm compared to the original thickness after the FsLDW treatment. The thinning of

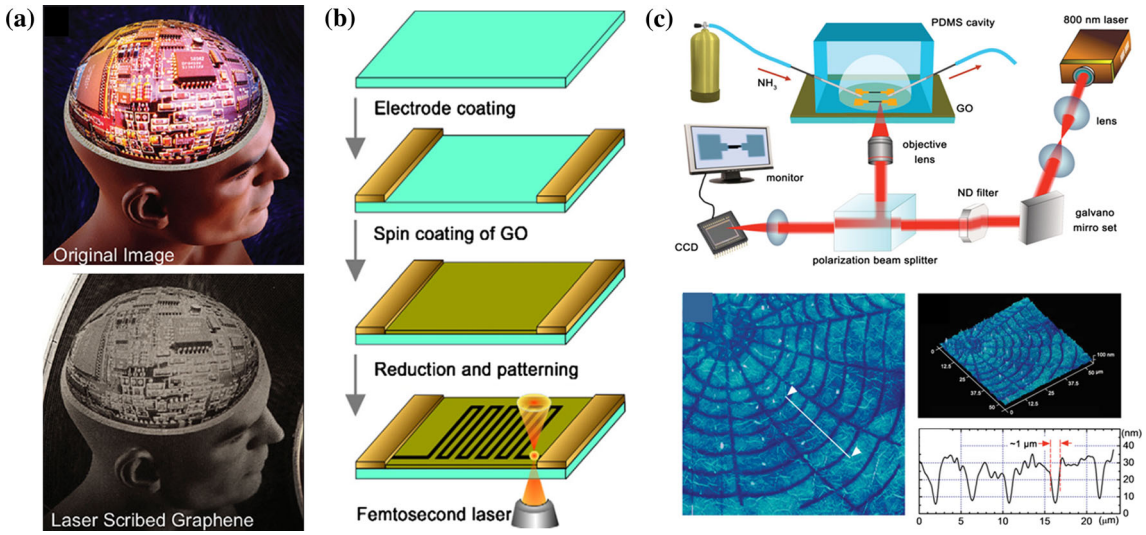

Figure 4 The NIR photoreduction of GO. **a** A complex colored original photograph (man's head) and the corresponding laser scribed graphene with different degree of photoreduction. Reprinted with permission from [89], copyright (2012) American Chemical Society. **b** Schematic diagram of RGO microcircuit with FsLDW technology. Reprinted with permission from [90], copyright (2010) Elsevier Ltd. c Schematic illustration of the preparation process of N-doped photoreduced GO and the AFM images of the processing samples. Reprinted with permission from [91], copyright (2014) Wiley-VCH.

GO film can be attributed to the compound PT effect caused by the electron excitation, which makes the loss of a part of the carbon materials in the laser scanning region and the production of CO_2, CO and H_2O [95].

Trusovas et al. [69] reported the picosecond pulsed irradiation was also a commonly used method for GO reduction, which exhibited more PT effect. Raman spectrum was selected to characterize the dependence of the reduction degree and the laser energy. Although several micrometers ribbon patterns of RGO have been exhibited, laser heating causes evaporation of volatile components in GO membrane materials, resulting in swelling of membrane materials. According to the temperature dynamic model, when the energy of the single pulse laser is 0.04 J cm^{-2} (50 mW), the surface temperature of the GO can be increased by 1400 °C for a number of nanoseconds. Then most of the hydroxyl, carboxyl and oxygen groups were removed. Unique morphology makes it achieve greater success in electronic fields, such as electrical energy storage applications.

It can be seen from the above that the photoreduction conditions of GO are not harsh. The are various methods although the mechanism is different. Actually, the reduction process can also be achieved easily under the illumination of solar light [66]. As a summary, Table 1 represents the details of GO photoreduction with different light sources. In general, the photoreduction is a kind of flexible, non-chemically modified, highly efficient, cost-effective and patterned method to regulate the properties of the surface/interface of GO films.

Potential application

In most cases, RGO films prepared by classical thermal or chemical methods are often seen as potential alternatives to graphene samples because of their comparable and similar features. Indeed, unlike the clumsy and small-scale mechanical exfoliated graphene preparation method, this facile prepared RGO can be applied to in various fields even for industrial production. Considering the superior characteristics of these methods, we have reasons to believe that photoreduction of GO will have an excellent prospect in the future.

Electrochemical (EC) energy storage devices

Li-ion batteries

Graphene is a relatively ideal electrode material as a good candidate for the Li-ion battery, because it is seized of a few excellent properties such as good electrical conductivity, large specific surface area,

Table 1 Different conditions of photoreduced GO and their typical applications

Light sources	Reduction and patterning manner[a]	Mechanism[b]	Atmosphere (catalysts)	Application	References
Extreme-UV laser (46.9 nm)	ULRP	PC	–	–	[76]
Excimer laser (248 nm)	ULRP	PT and PC	Vacuum	FETs	[75]
CW Raman laser (532 nm)	VLRP	PT and PC	Air, N_2	–	[80]
Nd:YAG laser (355 nm)	VLRP	PT and PC	Air	Humidity-sensing device; Biomimetic devices	[78, 127]
Diode laser (532 nm)	VLRP	PT and Thermal	Air	–	[86]
Diode laser (663 nm)	VLRP	PT	N_2	–	[87]
LightScribe technology (788 nm)	NILRP	PT	Air	Flexible electrodes; Supercapacitors	[89, 108]
FsLDW(790 nm)	NILRP	PT and PC	Air	Flexible electrodes; FETs	[90, 91, 118]
Picosecond pulsed laser irradiation (1064 nm)	NILRP	PT	N_2	–	[69]
Camera flash (400–800 nm)	VLIRP	PT	Air or N_2	Flexible electrodes; Li-ion batteries; Humidity-sensing device	[61, 71]
High-pressure Hg lamp (500 W)	ULIRP	PC	H_2 and N_2	Gas sensors	[79]
Focused sunlight	FSIRP	PT	Air	Actuator	[66]
Universal X-660 CO_2 laser	LDWRP	PT	Air	Supercapacitors	[109]
UV light	ULIRP	PT	Air	Actuator	[129]

[a]*ULRP* ultraviolet laser reduction and patterning, *VLRP* visible laser reduction and patterning, *NILRP* near-infrared laser reduction and patterning, *VLIRP* visible light irradiation for reduction and patterning, *ULIRP* ultraviolet light irradiation for reduction and patterning, *FSIRP* focused sunlight irradiation for reduction and patterning, *LDWRP* laser direct writing reduction and patterning

[b]*PT* photothermal reaction, *PC* photochemical reaction

strong mechanical strength and chemical–physical stability [66, 96]. As an electrode material, graphene is required to have a full contact with the electrolyte to make battery have a good cycle stability and a shorter path to charge and discharge (Fig. 5a) [97]. Thus, regarding the reduction of GO, it is very appropriate to develop a structure with high specific surface area. In addition, in order to facilitate the fabrication and integration of devices, the design of the patterns on macroscale can provide an opportunity to be realized. Flash-reduced GO anodes own unique "open-pore" structures as a result of the drastic expansion; Kaner et al. took advantage of this phenomenon for realizing efficient intercalation kinetics allows lithium ions to enter the underlying graphene sheets at a high rate [98]. Since GO contained plentiful OCGs, many methods can be used to carry out intense reduction treatments leading to porous and loose graphene structures. In addition,

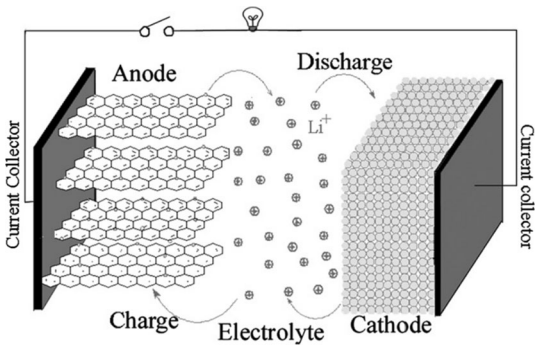

Figure 5 The schematic diagram of RGO-based Li-ion batteries. Reprinted with permission from [97], copyright (2009) the Royal Society of Chemistry.

the photothermally reduced GO anodes displayed excellent stability and cycling ability.

The ordered, patterned, nanostructured graphene electrodes can be obtained via photoreduction by using an appropriate optical mask. On the macro-dimension, the preparation of patterns is positive in

that it facilitates integration of more kinds of electronic devices. In the case of the Li-ion batteries themselves, the utilization of nanostructured materials with higher specific surface area could improve the energy storage capacity of the EC reaction. However, it must be pointed out that pure graphene is not the ideal electrode material for Li-ion batteries as compared with composite materials. By using appropriate material synthesis methods, active substances such as silicon, tin or aluminum have been placed in the gap of nanostructured graphene, thereby further enhancing the charge density of the device [99, 100].

Supercapacitors

Electrochemical (EC) supercapacitors have been widely concerned in energy storage technologies owning to their significantly higher power densities as compared to batteries [101–103]. The electrode materials determine the performance of the electrical parts, and the graphene and its derivatives are ideal electrode material for supercapacitors owning to their large surface area, mechanical strength and electrical properties. As a typical example, GO has been widely used in energy storage devices. The EC reaction mechanism of the supercapacitor is accompanied by an oxidation–reduction reaction [104–107]. The GO itself has a large number of OCGs even after the reduction step. At the same time, the preparation of a plate capacitor is an urgent need for the development of EC technologies. GO dissolved in water is the best candidate for an in-plane capacitor, convenient filming, patterning, and is highly convenient for the integration of complex patterning devices. El-Kady et al. [108] reported the production of RGO-based supercapacitors by using the laserscribing technique. This treatment can not only prepare complex patterns, but also produce a porous structure with surface area of 1520 m^2 g^{-1}.

Gao et al. [109] reported a novel fabrication method of microsupercapacitors on hydrated GO films by laser direct writing. They used a CO_2 laser to scan on GO film as a solid electrolyte and fabricated in-plane RGO electrodes with different designable micropatterns. Plentiful imprisoned water molecules in GO made this material both a good electrical insulator and ion transport medium, allowing it to serve as electrolyte and electrode separator in the whole device. Thus, a new type of all-carbon, monolithic supercapacitor was developed by laser reduction and patterning. Figure 6 shows schematics of CO_2 laser patterning of GO films to fabricate all graphene devices and their related EC performance. In particular, the capacitance–voltage (*C*–*V*) curves revealed a highest specific capacitance of ca. 0.51 mF cm^{-2} and a volumetric capacitance of ca. 3.1 F cm^{-3}.

Electronic devices

Owning to its ultra-high carrier mobility, high conductivity, transparency and excellent mechanical strength, graphene has emerged as a promising material for the development of the next generation of electronics such as electrodes and tuning layer [110, 111]. However, a series of challenges lies ahead to meet the need of fabrication of graphene-based electronics such as the regulation of the band gap and the preparation technology of the device [112, 113]. As an alternative material, GO holds promise for mass preparation, compatibility with any base and devisable patterning. For traditional thermal and chemical reduction methods of GO, on the other side, another shortcoming lies in the impossibility of using these materials to operate with flexible electronic devices such as PET (polyethylene terephthalate), PC (polycarbonate) and PMMA (polymethyl methacrylate), whereas the photoreduction strategies show obvious advantages [114–116]. For instance, making use of the nonthermal laser reduction technique, the Kymakis's group easily reduced a large area of GO spin-coated on flexible substrates, and the experiment showed that RGO sheet could be served as an electrode for organic photovoltaic cells [117].

Considering the accompanying process of photoinduction for GO and film-patterned design, the photoreduction, and the non-contact and mask-free characteristics, this method is ideal to fabricate practical graphene-based micro-electronic devices such as transparent electrodes, field-effect transistors (FETs) and sensors. As shown in Fig. 7, the preparation of FET devices has been realized by laser writing RGO microchannel between two pre-vaporized electrodes reported by Guo et al. [118]. In this work, the tunable bandgap of RGO microchannel resulting from laser reduction induced controlling of oxygen content studied from the first-principle were obtained. In detail, the bandgap of GO has been adjusted in the range of 2.4 to 0.9 eV by regulating and controlling the laser power. During this process,

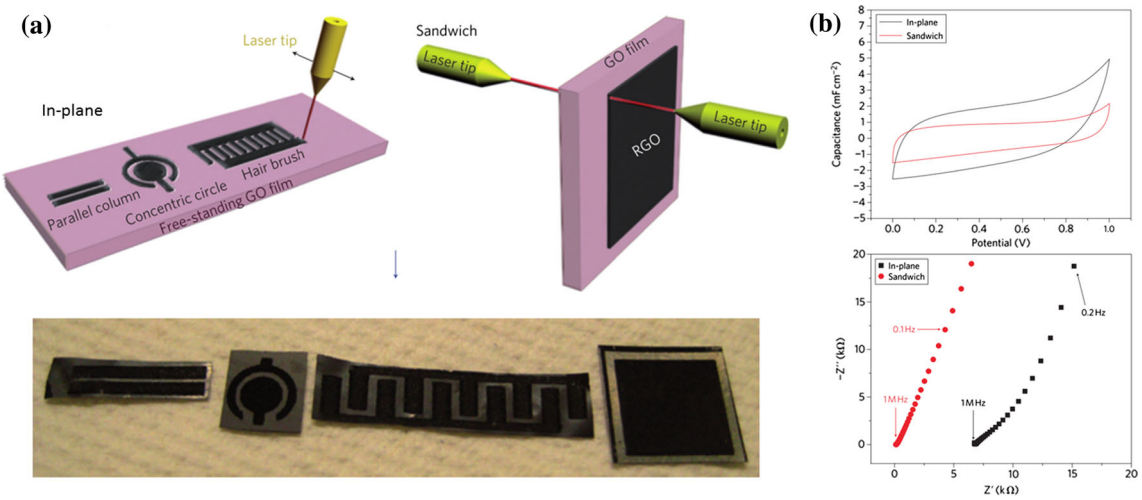

Figure 6 Schematics of CO_2 laser patterning of GO films to fabricate in-plane/sandwich RGO–GO–RGO devices (**a**) and EC behavior of devices (**b**). Reprinted with permission from [109], copyright (2011) Springer Nature.

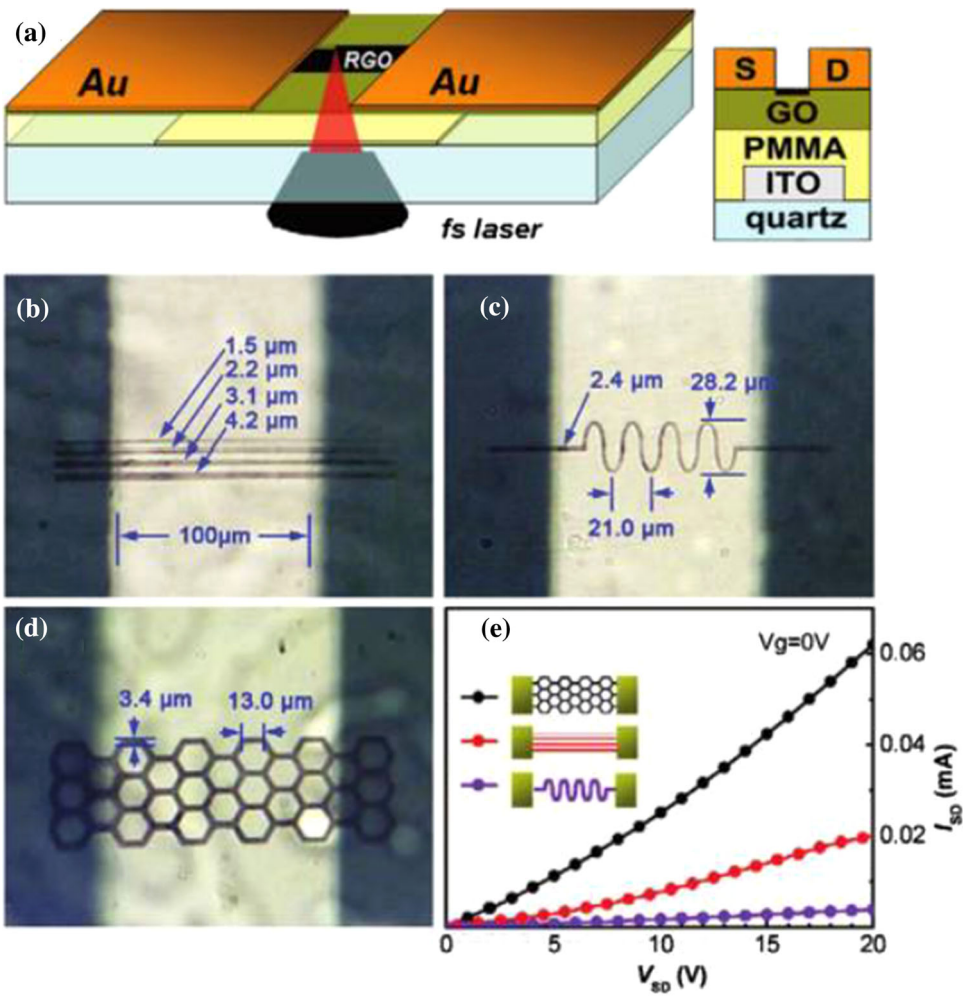

Figure 7 **a** Scheme of the RGO FET. Optical microscopic images of **b** parallel microlines with different width, **c** sinusoid and **d** hexagon grid was patterned between source and drain electrodes as a channel. **e** *I*–*V* curves of the above three channels with V_g = 0 V. Reprinted with permission from [118], copyright (2012) American Chemical Society.

they created desirable RGO patterned channels and fabricated the following bottom-gate graphene FETs successfully. The results revealed an on–off ratio of 56 by optimizing exciting laser energy at room temperature, implying the possibility of applying these devices in practice despite not fully meeting the technical indicators. Therefore, we are confident that the novel photoreduced GO containing ascendant bandgap-tunable feature can not only be used in the field of flexible micro-electronic devices, but also other graphene-based devices in the future.

Sensors

With the carbon atoms exposing to the external environment directly, graphene, the only single atom layer material, can act as electron donors or acceptors by absorbing or desorbing gaseous molecules effectively, which makes it a promising gas-sensing material [119, 120]. Recently, the graphene-based structures have been successfully verified to be sensitive to various gases, especially toxic aromatic compounds, just because of the uncommon electron transport characteristics on its surface. However, the graphene-based sensors would not be put into operation on a large scale unless graphene preparation methods become more convenient and the interaction with guest molecules becomes intense. Fortunately, thanks to plentiful hydrophilic OCGs on GO, the water-soluble attribute makes it a good alternative for both solution processing and interacting with sensing molecules [45, 48, 121]. By appropriate reduction treatment, the conductibility of GO can be improved, thereby allowing RGO to be regarded as potential active element for molecule detection. Additionally, the patterned graphene-based sensors were also developed for the improvement of the detection efficiency of various gases.

Unlike traditional reduction processes, the photoreduction of GO may be developed as a new method to exhibit outstanding features such as tunable conductivity, manipulative interactions with molecules and acceleration of adsorption/desorption. Previously, we reported a humidity-sensing device fabricated by camera flash treatment of GO [61]. When the GO film exposed to the flash, reduction and micronano-patterning have been occurred. That made the RGO areas conductive with the sheet resistance of 9.5 kΩ square^{-1} (GO: 2×10^8 Ω square^{-1}). Figure 8 shows the reduction of GO for sensing device and GO/other material composite for detection [61]. The response/recovery times of the sensors could be ascribed the interaction between H_2O molecules and RGO sheets. In addition, the hierarchical micro-nanosheets generated during the flash treatment made the interlayer RGO come out and promoted the sensing performance significantly.

Biomimetic devices

In the field of bionics, the wettability is described as the mutually exclusive physical properties between molecules of solid surface and the polar water molecule, which has been treated as a significant property characterizing the surface of the material [122, 123]. To imitate the biological template in nature, a large number of artificial bionic surfaces with balanced wettability described by steerable water contact angles (CAs) ranging from 0° to 150° above (superhydrophobic) have been readily fabricated [124]. Study on the wettability control of graphene surfaces has also been urgently carried out with the advent of graphene materials and the related development of various electronic devices have been pursued. GO also showed its value in the field of biomimetic materials. Experimental results showed that the water CA of the CVD graphene was ca. 95°, which is not in agreement with the calculation results considering a superhydrophobicity based on the 2D honeycomb structure [125]. It is not easy to directly and effectively tune the wettability of pristine graphene, while in the case of GO, the nature of the material itself allows to control its surface structure and chemical composition, thereby favoring operations [126].

The water CA of drying GO films is about 70°. The regulation of the wettability of GO is still facing two challenges. One is reducing the number of surface functional groups followed by the modulation of the surface energy. The other is changing of surface structure and increasing its roughness. Photoreduction of GO provides a convenient method to solve these two problems simultaneously. The reaction is accompanied by the integration of an ordered structure and pattern. For example, Jiang et al. fabricated periodically micronano-structured graphene films with grating and grid patterns that feature superhydrophobic wettability and rainbow color with the help of laser holography technique to simulate butterfly wings [127]. As shown in Fig. 9a, the presence

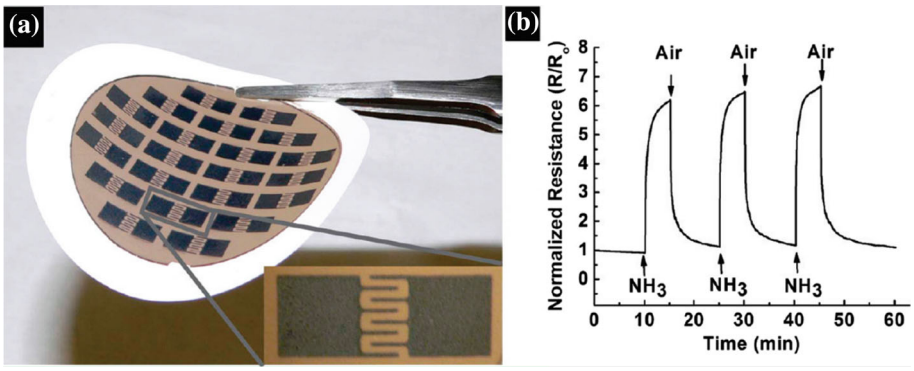

Figure 8 **a** Photographs of RGO/polystyrene interdigitated sensors. **b** The response performance of RGO sensor device exposed in 100 ppm of ammonia vapor. Reprinted with permission from [61], copyright (2009) American Chemical Society.

of double-periodical, ordered arrays of microstructure and layered nanostructure of the material itself make the graphene films having excellent superhydrophobity (Fig. 9b). Besides, the graphene films also exhibited transmission diffraction property and brilliant iridescence, due to which it could be directly observed by naked eyes (Fig. 9c–e). Considering these unique optical properties, it is predicted that these bionic films can be applied to some optoelectronic devices such as organic light emitting diodes and organic solar cells. The bioinspired graphene devices would be found to have broad application in the immediate future, such as tissue engineering which is proved by favorable biocompatibility of graphene and GO films in some previous reports.

Other applications

In addition to the above-mentioned applications, GO has also proved its value in other disciplines, actuators for instance. As previously mentioned, UV can reduce GO papers resulting in splendid RGO patterns through masking. However, the filtered GO paper has not completely reduced with circumscribed transmittance and heat transmission, yielding to the effect of self-coordinated photoreduction, the large-scale, programmable and arbitrary patterned GO/RGO bilayer structures have been fabricated in accordance with its natural tendency. Owing to the plentiful hydrophilic groups of GO, the double-layer structures show some sensitivity of humidity under air atmospheres [128]. As a result, they will bend

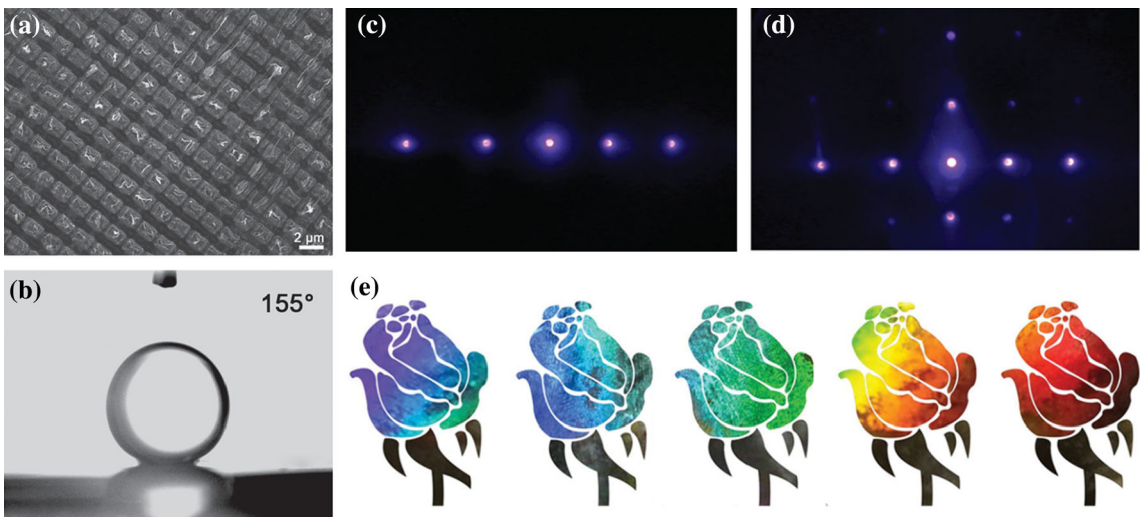

Figure 9 **a** SEM image of superhydrophobic graphene film. **b** Photograph of a water droplet on its surface, the CA is measured to be ≈ 155°. **c**–**e** Structural color and diffraction spots fired by laser with wavelength of 405 nm on the RGO film. Reprinted with permission from [127], copyright (2014) Wiley-VCH.

along the direction from GO to RGO, selectively absorbing more water in the GO layer as compared to the RGO layer. For this kind of bilayer structures, the response of curvature can be tuned by controlling the humidity. In order to better use the response characteristics of these materials, different patterns can be integrated for preparing functional components which can effectively convert the chemical energy in the material into mechanical energy, allowing convenient transport and movement of the devices.

The designable ideas and manufacturing of artificial actuators are inspired by the unique temperament of animals and plants in nature. Han et al. [129] prepared a smart graphene actuator by reducing RGO diagonal banded patterns on the GO banner paper with a UV masking which had been simulated tendril of the vines. As shown in Fig. 10a, the vine tentacles are spiral line which can stretch out or draw back freely and clamber over other plants vines. So the actuator with simple production presents unique humidity response characteristics. The GO/RGO ribbon bends into a certain curvature under room humidity and curl to helical shape under high humidity. Figure 10b shows a smart manipulator driven by the humidity can grab and put down any objects with appropriate size and mass. However, the releasing mechanical energy is equal to the change in the chemical energy in graphene materials under opposite humidity atmosphere environments. Here, the author put the graphene "tendril" on a plastic tube with adherency, on the one hand, to be a support for hand operation, on the other hand serve as a communication device connected to humidity atmosphere. By debugging the moisture, graphene manipulator can enwind slender objects under high humidity and release them in dry air. However, even if operational humidity–response graphene actuators could be readily realized through rational design of patterns of the GO/RGO bilayer structure, the development model of a graphene actuator is not unique. Thus, the development model is somewhat differently depending on the material, which gives us sufficient confidence to design and fabricate various smart actuators by incorporating unilateral UV photoreduction of GO paper and the laser lithography technique.

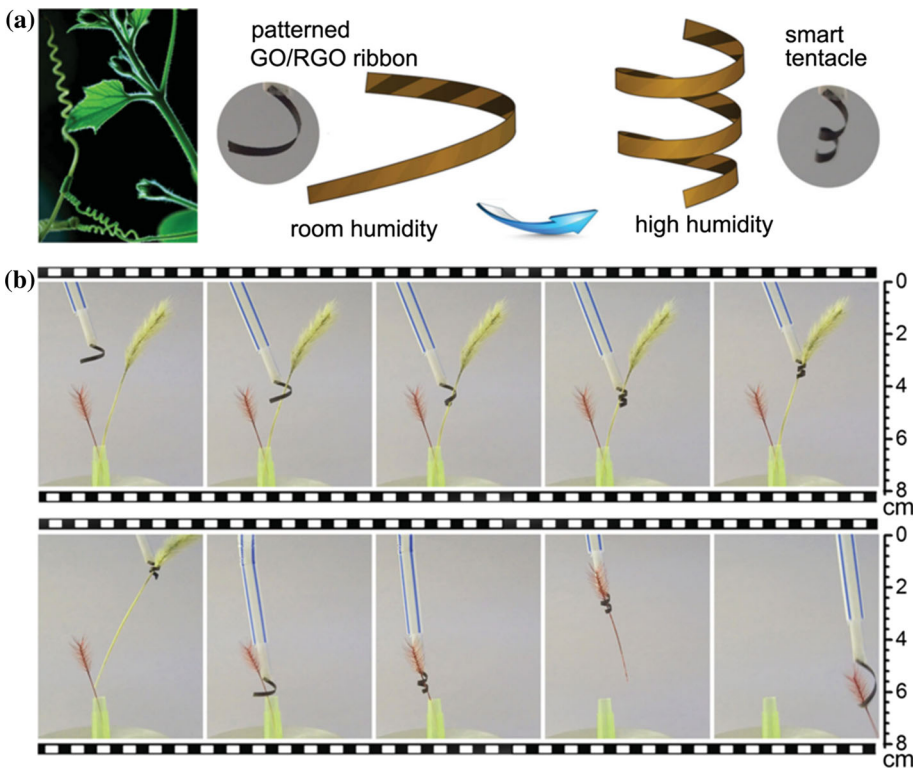

Figure 10 **a** Schematic illustration of smart graphene "tendril." **b** The smart graphene "tendril" was adhibited to a tube, which will make it grab and release objects under the humidity switch. Reprinted with permission from [129], copyright (2015) Wiley-VCH.

Conclusions and outlook

This review systematically summarizes series of photo-assisted methods for GO reduction and patterning. Different light source, such as laser, camera flash, UV lamp and focused sunlight, can be used as tools for reduction implementations, which mainly depends on the photon energy threshold at 3.2 eV. But most of the cases, considering the complexity of GO's chemical structure and the diverse emitting mechanism of different sources, the PT and PC processes play key roles during the reduction. Comparing with the traditional reduction methods, the photoreduction is distinguished for its accurate control of the graphitization degree, desirable patterning, integrative assembly, environmental friendless, economical and practical. So it endows unique advantages for development in various research fields including Li-ion batteries, supercapacitors, electronics and bio-sensing. However, the photoreduction still faces many challenges in the process of practice. One is the surface integrity control of materials during the light irradiation, and another is the large-area precise operation for industrial development. But we have sufficient reasons to believe that the photoreduction will certainly have more room for development in the future with the continuous progress of the novel theories and manufacturing technology,.

Acknowledgements

This work was supported by National Natural Science Foundation of China (NSFC) under Grants (51705192, 11804334); the China Postdoctoral Science Foundation (2017M611325); and the National Postdoctoral Program for Innovative Talents (BX201600064).

References

[1] Novoselov K, Geim A, Morozov S, Jiang D, Zhang Y, Dubonos S, Grigorieva I, Firsov A (2004) Electric field effect in atomically thin carbon films. Science 306:666–669

[2] Novoselov K, Jiang Z, Zhang Y, Morozov S, Stormer H, Zeitler U, Maan J, Boebinger G, Kim P, Geim A (2007) Room-temperature quantum hall effect in graphene. Science 315:1379

[3] Strek W, Cichy B, Radosinski L, Gluchowski P, Marciniak L, Lukaszewicz M, Hreniak D (2015) Laser-induced white-light emission from graphene ceramics—opening a band gap in graphene. Light Sci Appl 4:e237

[4] Rodrigo D, Tittl A, Limaj O, Abajo F, Pruneri V, Altug H (2017) Double-layer graphene for enhanced tunable infrared plasmonics. Light Sci Appl 6:e16277

[5] Shekhar C, Nayak A, Yan S et al (2015) Extremely large magnetoresistance and ultrahigh mobility in the topological weyl semimetal candidate Nbp. Nat Phys 11:645–649

[6] Hong J, Hu Z, Probert M (2015) Exploring atomic defects in molybdenum disulphide monolayers. Nat Commun 6:6293

[7] Ji L, Meduri P, Agubra V, Xiao X, Alcoutlabi M (2016) Graphene-based nanocomposites for energy storage. Adv Energy Mater 6:1502159

[8] Zheng Z, Li J, Ma T, Fang H et al (2017) Tailoring of electromagnetic field localizations by two dimensional graphene nanostructures. Light Sci Appl 6:e17057

[9] Blackburn J, Ferguson A, Cho C, Grunlan J (2018) Carbon-nanotube-based thermoelectric materials and devices. Adv Mater 30:1704386

[10] Guo Y, Xu G, Yang X et al (2018) Significantly enhanced and precisely modeled thermal conductivity in polyimide nanocomposites with chemically modified graphene via in situ polymerization and electrospinning-hot press technology. J Mater Chem C 6:3004–3015

[11] Zhu C, Han T, Duoss E, Golobic A, Kuntz J, Spadaccini C, Worsley M (2015) Highly compressible 3D periodic graphene aerogel microlattices. Nat Commun 6:6962

[12] Seyed H, Rouhollah J, Dorna E et al (2014) High-performance multifunctional graphene yarns: toward wearable all-carbon energy storage textiles. ACS Nano 8:2456–2466

[13] Lee H, Choi T, Lee Y et al (2016) A graphene-based electrochemical device with thermoresponsive microneedles for diabetes monitoring and therapy. Nat Nanotechnol 11:566–572

[14] Xin W, Chen X, Liu Z, Jiang W, Gao X, Jiang X, Chen Y, Tian J (2016) Photovoltage enhancement in twisted-bilayer graphene using surface plasmon resonance. Adv Opt Mater 4:1703–1710

[15] Xin W, Liu Z, Sheng Q et al (2014) Flexible graphene saturable absorber on two-layer structure for tunable mode-locked soliton fiber laser. Opt Express 22:10239–10247

[16] Zhu J, Yang D, Yin Z, Yan Q, Zhang H (2014) Graphene and graphene-based materials for energy storage applications. Small 10:3480–3498

[17] Diao S, Zhang X, Shao Z, Ding K, Jie J, Zhang X (2017) 12.35% efficient graphene quantum dots/silicon

heterojunction solar cells using graphene transparent electrode. Nano Energy 31:359–366

[18] Liu Z, Lau S, Yan F (2015) Functionalized graphene and other two-dimensional materials for photovoltaic devices: device design and processing. Chem Soc Rev 44:5638–5679

[19] Li Z, Huang H, Tang S et al (2016) Small gold nanorods laden macrophages for enhanced tumor coverage in photothermal therapy. Biomaterials 74:144–154

[20] Chimene D, Alge D, Gaharwar A (2015) Two dimensional nanomaterials for biomedical applications: emerging trends and future prospects. Adv Mater 27:7261–7284

[21] Xin W, Wu T, Zou T, Wang Y, Jiang W, Xing F, Yang J, Guo C (2019) Ultrasensitive optical detection of water pressure in microfluidics using smart reduced graphene oxide glass. Front Chem. https://doi.org/10.3389/fchem.2019.00395

[22] Huang B, Clark G, Navarro-Moratalla E et al (2017) Layer-dependent ferromagnetism in a van der Waals crystal down to the monolayer limit. Nature 546:270–273

[23] Wang C, Zhao M, Li J et al (2017) Silver nanoparticles/graphene oxide decorated carbon fiber synergistic reinforcement in epoxy-based composites. Polymer 131:263–271

[24] Geng P, Zheng S, Tang H, Zhu R, Zhang L, Cao S, Xue H, Pang H (2018) Transition metal sulfides based on graphene for electrochemical energy storage. Adv Energy Mater 8:1703259

[25] Li F, Zhou Z (2018) Micro/nanostructured materials for sodium ion batteries and capacitors. Small 14:1702961

[26] Dubal D, Chodankar N, Kim D, Gomez-Romero P (2017) Towards flexible solid-state supercapacitors for smart and wearable electronics. Chem Soc Rev 47:2065–2129

[27] Peng H, Huang J, Cheng X, Zhang Q (2017) Review on high-loading and high-energy lithium-sulfur batteries. Adv Energy Mater 7:1700260

[28] Trung T, Ramasundaram S, Hwang B, Lee N (2016) An all-elastomeric transparent and stretchable temperature sensor for body-attachable wearable electronics. Adv Mater 28:502–509

[29] Cheng Y, Wang R, Sun J, Gao L (2015) A stretchable and highly sensitive graphene-based fiber for sensing tensile strain, bending, and torsion. Adv Mater 27:7365–7371

[30] Liu H, Dong M, Huang W et al (2017) Lightweight conductive graphene/thermoplastic polyurethane foams with ultrahigh compressibility for piezoresistive sensing. J Mater Chem C 5:73–83

[31] Wang K, Ausri I, Chu K et al (2019) Pressure-driven solvent transport and complex ion permeation through graphene oxide membranes. Adv Mater Interfaces 6:1802056

[32] Ares P, Aguilar G, Rodriguez-San-Miguel D et al (2016) Mechanical isolation of highly stable antimonene under ambient conditions. Adv Mater 28:6332–6336

[33] Yi M, Shen Z (2015) A review on mechanical exfoliation for the scalable production of graphene. J Mater Chem A 3:11700–11715

[34] Coleman J (2013) Liquid exfoliation of defect-free graphene. Acc Chem Res 46:14–22

[35] Ismach A, Druzgalski C, Penwell S, Schwartzberg A, Zheng M, Javey A, Bokor J, Zhang Y (2010) Direct chemical vapor deposition of graphene on dielectric surfaces. Nano Lett 10:1542–1548

[36] Li X, Cai W, Colombo L, Ruoff R (2009) Evolution of graphene growth on Ni and Cu by carbon isotope labeling. Nano Lett 9:4268–4272

[37] Zhu F, Chen W, Xu Y et al (2015) Epitaxial growth of two-dimensional stanine. Nat Mater 14:1020–1025

[38] Dlubak B, Martin M, Deranlot C et al (2012) Highly efficient spin transport in epitaxial graphene on SiC. Nat Phys 8:557–561

[39] Ciesielski A, Samori P (2014) Graphene via sonication assisted liquid-phase exfoliation. Chem Soc Rev 43:381–398

[40] Ciesielski A, Haar S, Aliprandi A et al (2016) Modifying the size of ultrasound-induced liquid-phase exfoliated graphene: from nanosheets to nanodots. ACS Nano 10:10768–10777

[41] Lu L, Zhu Y, Shi C, Pei Y (2016) Large-scale synthesis of defect-selective graphene quantum dots by ultrasonic-assisted liquid-phase exfoliation. Carbon 109:373–383

[42] Chen Y, Gong X, Gai J (2016) Progress and challenges in transfer of large-area graphene films. Adv Sci 3:1500343

[43] Feng L, Wu L, Qu X (2013) New horizons for diagnostics and therapeutic applications of graphene and graphene oxide. Adv Mater 25:168–186

[44] Dimiev A, Alemany L, Tour J (2013) Graphene oxide origin of acidity, its instability in water, and a new dynamic structural model. ACS Nano 7:576–588

[45] Xu L, Shi R, Li H, Han C, Wu M, Wong C, Kang F, Li B (2018) Pseudocapacitive anthraquinone modified with reduced graphene oxide for flexible symmetric all-solid-state supercapacitors. Carbon 127:459–468

[46] Sherlala A, Raman A, Bello M, Asghar A (2017) A review of the applications of organo-functionalized magnetic graphene oxide nanocomposites for heavy metal adsorption. Chemosphere 193:1004–1017

[47] Wang J, Chen B (2015) Adsorption and coadsorption of organic pollutants and a heavy metal by graphene oxide and reduced graphene materials. Chem Eng J 281:379–388

[48] Yang Q, Su Y, Chi C et al (2017) Ultrathin graphene-based membrane with precise molecular sieving and ultrafast solvent permeation. Nat Mater 16:1198–1203

[49] Chen L, Shi G, Shen J et al (2017) Ion sieving in graphene oxide membranes via cationic control of interlayer spacing. Nature 550:380–383

[50] Zhuang L, Ge L, Yang Y, Li M, Jia Y, Yao X, Zhu Z (2017) Ultrathin iron–cobalt oxide nanosheets with abundant oxygen vacancies for the oxygen evolution reaction. Adv Mater 29:1606793

[51] Yousefi N, Sun X, Lin X et al (2014) Highly aligned graphene/polymer nanocomposites with excellent dielectric properties for high-performance electromagnetic interference shielding. Adv Mater 26:5480–5487

[52] Wen B, Wang X, Cao W et al (2014) Reduced graphene oxides: the thinnest and most lightweight materials with highly efficient microwave attenuation performances of the carbon world. Nanoscale 6:5754–5761

[53] Sun X, He J, Li G, Tang J, Wang T, Guo Y, Xue H (2012) Laminated magnetic graphene with enhanced electromagnetic wave absorption properties. J Mater Chem C 1:765–777

[54] Travlou N, Kyzas G, Lazaridis N, Deliyanni E (2013) Functionalization of graphite oxide with magnetic chitosan for the preparation of a nanocomposite dye adsorbent. Langmuir 29:1657–1668

[55] Sher S, Zhang K, Park A, Kim K, Park N, Park J, Yoo P (2013) Single-step solvothermal synthesis of mesoporous Ag–TiO_2–reduced graphene oxide ternary composites with enhanced photocatalytic activity. Nanoscale 5:5093–5101

[56] Thakur S, Karak N (2012) Green reduction of graphene oxide by aqueous phytoextracts. Carbon 50:5331–5339

[57] Lipatov A, Varezhnikov A, Wilson P, Sysoev V, Kolmakov A, Sinitskii A (2013) Highly selective gas sensor arrays based on thermally reduced graphene oxide. Nanoscale 5:5426–5434

[58] Feng H, Cheng R, Zhao X, Duan X, Li J (2013) Corrigendum: a low-temperature method to produce highly reduced graphene oxide. Nat Commun 4:1539

[59] Kuila T, Mishra A, Khanra P, Kim N, Lee J (2013) Recent advances in the efficient reduction of graphene oxide and its application as energy storage electrode materials. Nanoscale 5:52–71

[60] Pei S, Cheng H (2012) The reduction of graphene oxide. Carbon 50:3210–3228

[61] Cote L, Cruz-Silva R, Huang J (2009) Flash reduction and patterning of graphite oxide and its polymer composite. J Am Chem Soc 131:11027–11032

[62] Gilje S, Dubin S, Badakhshan A, Farrar J, Danczyk S, Kaner R (2010) Photothermal deoxygenation of graphene oxide for patterning and distributed ignition applications. Adv Mater 22:419–423

[63] Williams G, Seger B, Kamat P (2008) TiO_2-graphene nanocomposites UV-assisted photocatalytic reduction of graphene oxide. ACS Nano 2:1487–1491

[64] Ng Y, Iwase A, Kudo A, Amal R (2010) Reducing graphene oxide on a visible-light $BiVO_4$ photocatalyst for an enhanced photoelectrochemical water splitting. J Phys Chem Lett 1:2607–2612

[65] Mukherjee R, Thomas A, Krishnamurthy A, Koratkar N (2012) Photothermally reduced graphene as high-power anodes for lithium-ion batteries. ACS Nano 6:7867–7878

[66] Han D, Zhang Y, Jiang H, Xia H, Feng J, Chen Q, Xu H, Sun H (2015) Moisture-responsive graphene paper prepared by self-controlled photoreduction. Adv Mater 27:332–338

[67] Cai J, Lv C, Aoyagi E, Ogawa S, Watanabe A (2018) Laser direct writing of a high-performance all-graphene humidity sensor working in a novel sensing mode for portable electronics. ACS Appl Mater Interfaces 10:23987–23996

[68] Zheng X, Jia B, Chen X, Gu M (2014) In situ third-order non-linear responses during laser reduction of graphene oxide thin films towards on-chip non-linear photonic devices. Adv Mater 26:2699–2703

[69] Trusovas R, Ratautas K, Račiukaitis G, Barkauskas J, Stankevičienė I, Niaura G, Mažeikienė R (2013) Reduction of graphite oxide to graphene with laser irradiation. Carbon 52:574–582

[70] Chen W, Li S, Chen C, Yan L (2011) Self-assembly and embedding of nanoparticles by in situ reduced graphene for preparation of a 3D graphene/nanoparticle aerogel. Adv Mater 23:5679–5683

[71] Abdelsayed V, Moussa S, Hassan H, Aluri H, Collinson M, El-Shall M (2010) Photothermal deoxygenation of graphite oxide with laser excitation in solution and graphene-aided increase in water temperature. J Phys Chem Lett 1:2804–2809

[72] Kim S, Parvez M, Chhowalla M (2009) UV-reduction of graphene oxide and its application as an interfacial layer to reduce the back-transport reactions in dye-sensitized solar cells. Chem Phys Lett 483:124–127

[73] Ding Y, Zhang P, Zhuo Q, Ren H, Yang Z, Jiang Y (2011) A green approach to the synthesis of reduced graphene oxide nanosheets under UV irradiation. Nanotechnology 22:215601

[74] Sokolov D, Rouleau C, Geohegan D, Orlando T (2013) Excimer laser reduction and patterning of graphite oxide. Carbon 53:81–89

[75] Arul R, Oosterbeek R, Robertson J, Xu G, Jin J, Simpson M (2016) The mechanism of direct laser writing of

graphene features into graphene oxide films involves photoreduction and thermally assisted structural rearrangement. Carbon 99:423–431

[76] Prezioso S, Perrozzi F, Donarelli M, Bisti F, Santucci S, Palladino L, Nardone M, Treossi E et al (2012) Large area extreme-UV lithography of graphene oxide via spatially resolved photoreduction. Langmuir 28:5489–5495

[77] Smirnov V, Arbuzov A, Shul'ga Y, Baskakov S, Martynenko V, Muradyan V, Kresova E (2011) Photoreduction of graphite oxide. High Energy Chem 45:57–61

[78] Guo L, Jiang H, Shao R et al (2012) Two-beam-laser interference mediated reduction, patterning and nanostructuring of graphene oxide for the production of a flexible humidity sensing device. Carbon 50:1667–1673

[79] Matsumoto Y, Koinuma M, Kim S, Watanabe Y, Taniguchi T, Hatakeyama K, Tateishi H, Ida S (2010) Simple photoreduction of graphene oxide nanosheet under mild conditions. ACS Appl Mater Interfaces 2:3461–3466

[80] Sokolov D, Shepperd K, Orlando T (2010) Formation of graphene features from direct laser-induced reduction of graphite oxide. J Phys Chem Lett 1:2633–2636

[81] Wang L, Lin X, Hu W et al (2015) Broadband tunable liquid crystal terahertz waveplates driven with porous graphene electrodes. Light Sci Appl 4:e342

[82] Dai Z, Xiao X, Wu W et al (2015) Plasmon-driven reaction controlled by the number of graphene layers and localized surface plasmon distribution during optical excitation. Light Sci Appl 4:e253

[83] Chen J, Zheng B, Shao G et al (2015) An all-optical modulator based on a stereo graphene–microfiber structure. Light Sci Appl 4:e360

[84] Zhu L, Liu F, Lin H et al (2016) Angle-selective perfect absorption with two dimensional materials. Light Sci Appl 5:e16052

[85] Xu Q, Ma T, Danesh M et al (2017) Effects of edge on graphene plasmons as revealed by infrared nanoimaging. Light Sci Appl 6:e16204

[86] Fatt T, Tao Y, Soon T, Wei H, Haur S (2012) Direct laser-enabled graphene oxide-reduced graphene oxide layered structures with micropatterning. J Appl Phys 112:064309

[87] Zhou Y, Bao Q, Varghese B, Tang L, Tan C, Sow C, Loh K (2010) Microstructuring of graphene oxide nanosheets using direct laser writing. Adv Mater 22:67–71

[88] Avella-oliver M, Morais S, Puchades R, Maquieira A (2016) Towards photochromic and thermochromic biosensing. TrAC Trends Anal Chem 79:37–45

[89] Strong V, Dubin S, El-Kady M, Lech A, Wang Y, Weiller B, Kaner R (2012) Patterning and electronic tuning of laser scribed graphene for flexible all-carbon devices. ACS Nano 6:1395–1403

[90] Zhang Y, Guo L, Wei S, He Y, Xia H, Chen Q, Sun H, Xiao F (2010) Direct imprinting of microcircuits on graphene oxides film by femtosecond laser reduction. Nano Today 5:15–20

[91] Guo L, Zhang Y, Han D et al (2014) Laser-mediated programmable N doping and simultaneous reduction of graphene oxides. Adv Opt Mater 2:120–125

[92] Kim G, Shao L, Zhang K (2013) Engineered doping of organic semiconductors for enhanced thermoelectric efficiency. Nat Mater 12:719–723

[93] Dianov E (2012) Bismuth-doped optical fibers: a challenging active medium for near-IR lasers and optical amplifiers. Light Sci Appl 1:e12

[94] Xing G, Yi J, Yan F, Wu T, Li S (2014) Positive magnetoresistance in ferromagnetic Nd-doped In_2O_3 thin films grown by pulse laser deposition. Appl Phys Lett 104:202411

[95] Park S, An J, Potts J, Velamakanni A, Murali S, Ruoff R (2011) Hydrazine-reduction of graphite-and graphene oxide. Carbon 49:3019–3023

[96] Reddy A, Srivastava A, Gowda S, Gowda S, Gullapalli H, Dubey M, Ajayan P (2010) Synthesis of nitrogen-doped graphene films for lithium battery application. ACS Nano 4:6337–6342

[97] Liang M, Zhi L (2009) Graphene-based electrode materials for rechargeable lithium batteries. J Mater Chem 19:5871–5878

[98] Zhao X, Hayner C, Kung M, Kung H (2012) Photothermal-assisted fabrication of iron fluoride–graphene composite paper cathodes for high-energy lithium-ion batteries. Chem Commun 48:9909–9911

[99] Wang W, Song X, Gu C, Liu D, Liu J, Huang J (2018) A high-capacity $NiCo_2O_4$@reduced graphene oxide nanocomposite Li-ion battery anode. J Alloy Compd 741:223–230

[100] Wang G, Zhang J, Yang S, Wang F, Zhuang X, Müllen K, Feng X (2018) Vertically aligned MoS_2 nanosheets patterned on electrochemically exfoliated graphene for high-performance lithium and sodium storage. Adv Energy Mater 8:1702254

[101] Kötz R, Carlen M (2000) Principles and applications of electrochemical capacitors. Electrochim Acta 45:2483–2498

[102] Wei W, Cui X, Chen W, Ivey D (2011) Manganese oxide-based materials as electrochemical supercapacitor electrodes. Chem Soc Rev 40:1697–1721

[103] Chen H, Cong T, Yang W, Tan C, Li Y, Ding Y (2009) Progress in electrical energy storage system: a critical review. Prog Nat Sci 19:291–312

[104] Kaempgen M, Chan C, Ma J, Cui Y, Gruner G (2009) Printable thin film supercapacitors using single-walled carbon nanotubes. Nano Lett 9:1872–1876
[105] Dong X, Xu H, Wang X et al (2012) 3D graphene–cobalt oxide electrode for high-performance supercapacitor and enzymeless glucose detection. ACS Nano 6:3206–3213
[106] Yan J, Wang Q, Wei T, Fan Z (2014) Recent advances in design and fabrication of electrochemical supercapacitors with high energy densities. Adv Energy Mater 4:1300816
[107] Yu Z, Tetard L, Zhai L, Thomas J (2015) Supercapacitor electrode materials: nanostructures from 0 to 3 dimensions. Energy Environ Sci 8:702–730
[108] El-Kady M, Strong V, Dubin S, Kaner R (2012) Laser scribing of high-performance and flexible graphene-based electrochemical capacitors. Science 335:1326–1330
[109] Gao W, Singh N, Song L et al (2011) Direct laser writing of micro-supercapacitors on hydrated graphite oxide films. Nat Nanotechnol 6:496–500
[110] Fu L, Wang A, Lai G et al (2018) A glassy carbon electrode modified with N-doped carbon dots for improved detection of hydrogen peroxide and paracetamol. Mikrochim Acta 185:87
[111] Wang X, Ouyang Y, Li X, Wang H, Guo J, Dai H (2008) Room-temperature all-semiconducting sub-10-nm graphene nanoribbon field-effect transistors. Phys Rev Lett 100:206803
[112] Zhang Y, Tang T, Girit C, Hao Z, Martin M, Zettl A, Crommie M, Shen Y et al (2009) Direct observation of a widely tunable bandgap in bilayer graphene. Nature 459:820–823
[113] Ni Z, Yu T, Lu Y, Wang Y, Feng Y, Shen Z (2008) Uniaxial strain on graphene: Raman spectroscopy study and band-gap opening. ACS Nano 2:2301–2305
[114] Ghosh D, Lim J, Narayan R, Kim S (2016) High energy density all solid state asymmetric pseudocapacitors based on free standing reduced graphene oxide-Co_3O_4 composite aerogel electrodes. ACS Appl Mater Interfaces 8:22253–22260
[115] Feng L, Wang K, Zhang X, Sun X, Li C, Ge X, Ma Y (2018) Flexible solid-state supercapacitors with enhanced performance from hierarchically graphene nanocomposite electrodes and ionic liquid incorporated gel polymer electrolyte. Adv Funct Mater 28:1704463
[116] Wang Q, Jian M, Wang C, Zhang Y (2017) Carbonized silk nanofiber membrane for transparent and sensitive electronic skin. Adv Funct Mater 27:1605657
[117] Kymakis E, Savva K, Stylianakis M, Fotakis C, Stratakis E (2013) Flexible organic photovoltaic cells with in situ nonthermal photoreduction of spin-coated graphene oxide electrodes. Adv Funct Mater 23:2742–2749
[118] Guo L, Shao R, Zhang Y (2012) Bandgap tailoring and synchronous microdevices patterning of graphene oxides. J Phys Chem C 116:3594–3599
[119] Meng F, Zheng H, Chang Y, Zhao Y, Li M, Wang C, Sun Y, Liu J (2018) One-step synthesis of Au/SnO_2/RGO nanocomposites and their VOC sensing properties. IEEE T Nanotechnol 17:212–219
[120] Tian H, Fan H, Ma J, Liu Z, Ma L, Lei S, Fang J, Long C (2018) Pt-decorated zinc oxide nanorod arrays with graphitic carbon nitride nanosheets for highly efficient dual-functional gas sensing. J Hazard Mater 341:102–111
[121] Wang T, Huang D, Yang Z, Xu S, He G, Li X, Hu N, Yin G et al (2016) A review on graphene-based gas/vapor sensors with unique properties and potential applications. Nanomicro Lett 8:95–119
[122] Wong T, Kang S, Tang S, Smythe E, Hatton B, Grinthal A, Aizenberg J (2011) Bioinspired self-repairing slippery surfaces with pressure-stable omniphobicity. Nature 477:443–447
[123] Zheng Y, Bai H, Huang Z, Tian X, Nie F, Zhao Y, Zhai J, Jiang L (2010) Directional water collection on wetted spider silk. Nature 463:640–643
[124] Yao X, Song Y, Jiang L (2011) Applications of bio-inspired special wettable surfaces. Adv Mater 23:719–734
[125] Feng L, Li S, Li Y et al (2003) Super-hydrophobic surfaces: from natural to artificial. Adv Mater 14:1857–1860
[126] Li X, Reinhoudt D, Crego-Calama M (2007) What do we need for a superhydrophobic surface? A review on the recent progress in the preparation of superhydrophobic surfaces. Chem Soc Rev 36:1350–1368
[127] Jiang H, Zhang Y, Han D, Xia H, Feng J, Chen Q, Hong Z, Sun H (2014) Bioinspired fabrication of superhydrophobic graphene films by two-beam laser interference. Adv Funct Mater 24:4595–4602
[128] Cheng H, Liu J, Zhao Y, Hu C, Zhang Z, Chen N, Jiang L, Qu L (2013) Graphene fibers with predetermined deformation as moisture-triggered actuators and robots. Ange Chem Int Ed 52:10482–10486
[129] Han D, Zhang Y, Liu Y et al (2015) Bioinspired graphene actuators prepared by unilateral UV irradiation of graphene oxide papers. Adv Funct Mater 25:4548–4557